Assessing Soybean Water Stress Patterns And Enso Occurrence In Southern Brazil: An In Silico Approach

Gabriel da R. Hintz[1], Ana Carcedo[1], Luiz Felipe A. Almeida[1], Tiago A. N. Horbe[2], Geomar Corassa[2], Luan Pott[3], Trevor Hefley[4], and Ignacio Ciampitti[1].

[1]Department of Agronomy, Kansas State University, United States

[2] Cooperativa Central Gaucha Ltda, Brazil

[3]Grupo Don Mario, Brazil

[4]Department of Statistics, Kansas State University, United States

A paper from the Proceedings of the
16th International Conference on Precision Agriculture
21-24 July 2024
Manhattan, Kansas, United States

Abstract.

Soybeans are a crucial crop for global food security, yet climate instability, particularly water stress (WS), is a major concern. This study aims to explore this constrain via an in-silico approach to characterize water stress and spatial patterns and their frequency within ENSO events; and evaluate climate-adaptative strategies (planting dates and maturity groups) associated with ENSO events to mitigate crop failure risk and maximize yield. With this aim, APSIM Next Generation was employed to simulate three widely used maturity groups (MG, 5.0, 5.8, and 6.4) and eight planting dates (from October 5th to January 20th) over 30 years across 187 locations in RS, Brazil. Four regions were delineate: Northeast (NE), North (N), Central (C), and Southwest (SW) and four WS patterns were defined (no stress, early stress, late stress, and whole season stress). Water stress patterns varied across regions, with the SW region experiencing more frequent and severe stress (up to 50% of whole season stress during La Nina), with an overall WS yield reduction up to 2 Mg ha-1 (~50%). The MG 5.0 resulted in higher failure risk across all regions. Early planting dates resulted in the highest yield variability (up to 5 Mg ha^{-1}). Adaptive management strategies, such as optimizing planting dates and maturity groups, are crucial to mitigate yield penalties and failure risk.

Keywords.
Water stress, Soybean, ENSO, Crop modeling.

Introduction

Brazil plays a critical role as the principal soybean producer in the world (FAO, 2024). In this context, the state of Rio Grande do Sul (RS, located in the southern part of Brazil) is particularly noteworthy, contributing to roughly 15% of Brazil's total soybean planted area (CEPEA, 2024; CONAB, 2024). However, a major concern in RS is the large interannual yield variability, mainly attributed to climate instability (Sentelhas et al., 2015). Rio Grande do Sul is especially vulnerable to water stress as most farming systems are conducted under dryland conditions (~98%; Martins et al., 2021). Therefore, seasonal variations in precipitation and temperature significantly impact soybean yields, underscoring the urgent need for developing climate-adaptative management strategies (Kukal and Irmak, 2018; Lobell et al., 2011; Mourtzinis et al., 2015; Rezaei et al., 2023). This context delineates an evident research gap in understanding the effect of weather patterns and their influence on soybean production (Ray et al., 2015). Considering this, the El Niño Southern Oscillation (ENSO) has profound effects on weather patterns globally, including Southern Brazil (Cai et al., 2020; Cirino et al., 2015; Lin and Qian, 2019; Nóia Júnior et al., 2020; Nóia Júnior and Sentelhas, 2019), and can be used to predict rainfall and temperature variation (Iizumi et al., 2014; Ropelewski & Halpert, 1987). Particularly in Brazil, numerous studies have documented the adaptation of crop management practices to prevailing environmental conditions, employing crop modeling as a foundational tool for assisting the farming decision-making process (Battisti et al., 2020b, 2017; Battisti & Sentelhas, 2019; Figueiredo Moura da Silva et al., 2021; Peterson et al., 2020). However, to the extent of our knowledge, limited efforts have been made to connect seasonal stress patterns with the ENSO phases and their management implications.

This study aimed to calibrate and validate soybean varieties using the APSIM model, across a wide range of environmental conditions. The research utilized two independent datasets to address the challenges of water stress and climate variability on soybean production in RS, Brazil. The specific objectives were to: 1) characterize water stress and spatial patterns, and their frequency within ENSO events using an in-silico approach, and 2) explore planting dates and maturity groups as climate-adaptive strategies associated with ENSO events to mitigate crop failure risk.

Methods

This publication is an adaptation of Hintz et al. (under preparation).

Soybean growth simulation

Simulations covered the three soybean cultivars across eight planting dates (15 days apart each one - from October 5th to January 20th), representing the typical sowing window for RS (CONAB, 2022), and to cover the environmental variability within the area, a point-grid was set targeting 200 points equally spaced from each other to compose the locations. We removed 13 locations due to the lack of either soil or weather information, ending up with 187 locations set up in a grid pattern separated by 39 km in longitude and 33 km in latitude. The simulations were performed setting the sowing density at 30 plants m^{-2}. Daily precipitation was downloaded from CHIRPS (Funk et al., 2015), maximum and minimum temperature, and radiation were downloaded from NASAPOWER, and soil data was retrieved from and SoilGrids (“ISRIC — World Soil Information”; Poggio et al., 2021; Turek et al., 2023; Pott et al., 2022). We chose CHIRPS over NASAPOWER for precipitation data, given its superior resolution. At the start of the simulation, wheat residue (4 Mg ha-1) was added as soil cover, reflecting the widespread adoption of no-till farming in the region (Conab, 2024; Fuentes-Llanillo et al., 2021).

Water stress and environmental type classification

The model was set to simulate daily water stress (WS), accumulated thermal time, phenology, and seed yield. The WS was assessed from the ratio between the potential soil water supply and the crop transpiration demand (Robertson et al., 2002). The WS factor was averaged for every

100 °Cd of thermal time, following Chapman et al. (2000), with the early grain filling phenological stage centered as the reference, therefore, negative values of thermal time represent phenological states prior early grain filling while positive values represent phenological stages after early grain filling. The water stress patterns were clustered employing simulations for the whole region and the historical weather serie.

Spatial clustering

Spatially homogeneous regions with similar yield responses to planting dates and MG. Mean yield and its coefficient of variation were computed to quantify central tendency and dispersion, respectively, and used to assess relative variability for each combination of location, planting date, and cultivar. The Spatial Fuzzy c-means (SFCM) algorithm from the *geocmeans* package (Jeremy, 2023), was employed. The SFCM algorithm was parameterized with four clusters (k = 4), a fuzziness coefficient of 3 (m = 3), and a spatial penalty parameter of 2 (alpha = 2). The algorithm was set to perform data standardization internally and utilized a median-based lag method to incorporate spatial dependency. All the steps above were performed using the statistical programming language R (R Core Team, 2024).

El Niño Southern Oscillation

The crop seasons were classified into El Niño Southern Oscillation phases, based on the National Oceanic and Atmospheric Administration (NOAA). This classification employs the Pacific Ocean sea surface temperature anomaly (SSTA) in relation to the normal in the El Niño 3.4 region. A given growing season was classified as El Niño when the mean SSTA is equal to or above 0.5 °C for the period between October and April. When the SSTA was equal to or below -0.5 °C for the period between October and April it was considered La Niña. A Neutral year was characterized when the SSTA remained between -0.5 and 0.5 °C.

Failure risk

The failure risk was established by the percentage of simulations that yielded less than the economic break-even soybean yield in a given scenario. The economic break-even yield was estimated by averaging the ratio between the cost of production (985 \$ ha^{-1}) and the grain average price (441 \$ Mg^{-1}) of the respective season for the last five seasons (2019/2020 – 2023/2024) (CONAB, 2024).

Statistical Analysis

A linear mixed-effects model was applied to assess the management impact on yield. The interaction among planting date, cultivar, and ENSO were treated as fixed effects, while the season with the location nested within the season was treated as the random effect. The crop yield was the response variable. This model was fitted using the *lme4* R package (Bates et al., 2015). To ensure the validity of our model, the standardized residuals were compared against the fitted values to check for the assumptions of normality and equal variance (Zuur et al., 2009). An ANOVA test with type III sum of squares was employed to test treatment effects, through the *car* package (Fox and Weisberg, 2018). All steps of the statistical analysis were carried out using the R software (R Core Team, 2024).

Results

Spatial clustering, water stress, environmental type classification, and soybean yield dynamics

Four distinct water stress (WS) patterns were identified: no stress (WS factor above 0.75), early stress (WS factor around 0.5 at 500 degree-days before flowering), late stress (WS factor around 0.5 at flowering), and whole-season stress (WS factor below 0.5 from 400 degree-days before flowering to 200 degree-days after flowering) (Fig. 1). Whole-season stress led to a significant

reduction in seed yield, up to 50% (~2 Mg ha^{-1}) compared to no stress (~4 Mg ha^{-1}). Both early and late stress conditions resulted in intermediate average yields of around 3 Mg ha-1 (Fig. 1). Based on yield performance, four regions were classified: Northeast (NE), North (N), Central (C), and Southwest (SW) (Fig. 1). The average seed yield was 4.1, 3.4, 3.0, and 2.7 Mg ha^{-1}, with a coefficient of variation (CV) of 25%, 26%, 29%, and 33% for the regions NE, N, C, and SW, respectively (Fig. 1). The most productive region, NE, had the highest frequency of the no stress pattern (~66%) and only 5% occurrence of whole-season stress in simulations. Conversely, the least productive region, SW, experienced whole-season stress in one-third of the simulations.

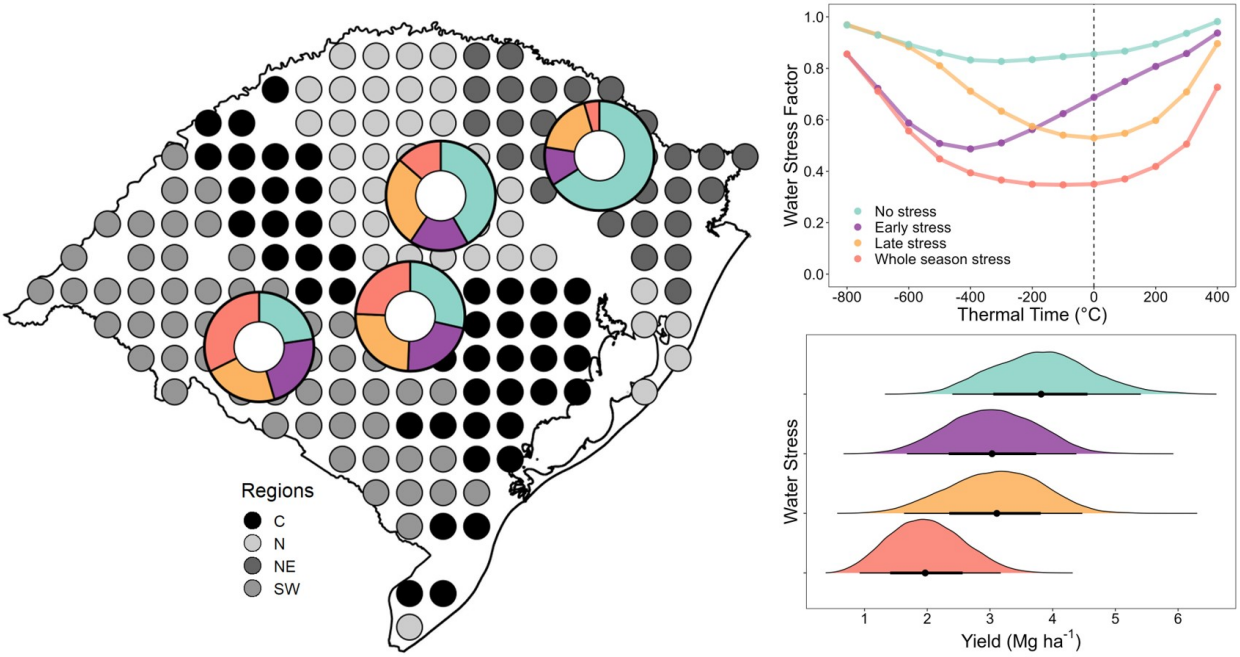

Figure 1. Soybean water stress patterns, clustered regions, and yield response. Water stress patterns (top-right). The relationship between water stress factor and crop development (thermal time). The vertical dashed line represents the early grain-filling phenological stage; Soybean yield (bottom-right). The distribution of soybean yield under varying water stress conditions; Clustered regions (left). The pie charts on the map, varying in color and size, represent the relative frequency of four categorized water stress patterns: no stress (green), early stress (purple), late stress (orange), and whole season stress (red) within each region; (C) distribution of soybean yields across the Southwest (SW), Central (C), North (N), and Northeast (NE) regions. Adapted from Hintz et al., (under preparation).

Water stress and ENSO frequency

Over the past three decades, the average seasonal ENSO phases have been distributed as follows: 41% La Niña, 31% Neutral, and 28% El Niño. Although El Niño events were the least frequent, they were characterized by a predominant no-stress pattern across regions, with frequencies of 90%, 81%, 56%, and 45% in the NE, N, C, and SW regions, respectively. In contrast, La Niña events were associated with a higher frequency of whole-season stress in the C (35%) and SW (50%) regions. During Neutral events, under stress scenarios, the probability of late stress was higher compared to whole-season and early stress. The NE region exhibited a prevailing pattern of no stress across all ENSO phases (over 70%), with whole-season stress rarely occurring (2%). In the N region, most Neutral seasons featured either no stress (40%) or late stress (37%).

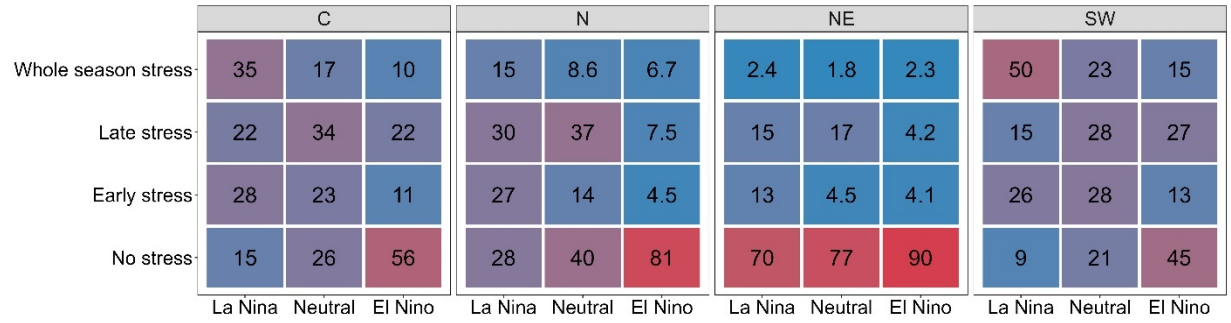

Figure 2. Frequency of water stress patterns across four regions during La Niña, Neutral, and El Niño phases. The heatmap conveys the percentage of stress occurrences, with color intensity indicating frequency. Adapted from Hintz et al., (under preparation).

Failure risk

The calculated economic break-even yield was 2.2 Mg ha^{-1}. In the C region, the average failure risk probabilities during El Niño, Neutral, and La Niña events were 13%, 16%, and 30%, respectively, while the N region had lower probabilities at 7%, 8%, and 12%. The SW region presented higher probabilities of 21%, 20%, and 48%. Conversely, the NE region maintained a consistently low failure chance of less than 3% for all ENSO phases. ENSO led to a ~15% and 30% increase in crop failure risk in the C and SW regions during La Niña events, compared to Neutral and El Niño seasons, which followed similar failure risk patterns (Fig. 3A). The shortest maturity group (MG) resulted in the greatest failure risks in all regions during La Niña events, reaching 40% to 50% failure risk in the SW and C regions. In comparison, MGs 5.8 and 6.4 reported a reduced failure risk by approximately 10% to 15%. These two MGs showed similar failure risks across regions and ENSO phases (Fig. 3B). Regarding planting dates, there was an increasing failure risk for the C and SW regions as planting was delayed during El Niño and Neutral events, peaking in late January. In contrast, the NE region's failure risk remained flat and under 10% for all planting dates. La Niña events differed from Neutral and El Niño events mainly during early planting dates, resulting in higher failure risk compared to these events, reaching over 50% risk in the SW region for October planting dates, for example (Fig. 3C).

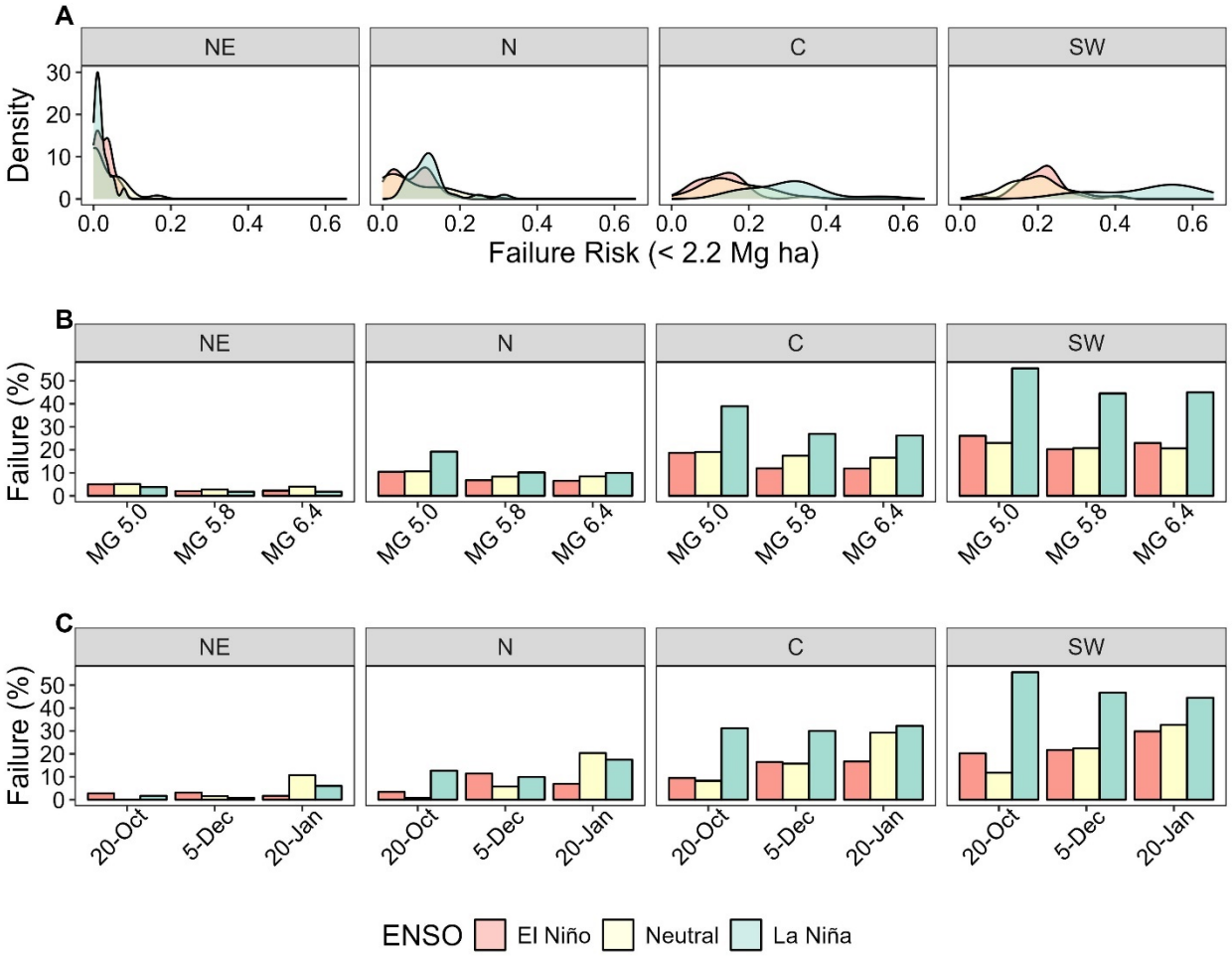

Figure 3. Comparative descriptive analysis of crop failure risk across different ENSO phases (colors): (A) Probability density functions for the four regions (panels) showing risk distribution under El Niño, Neutral, and La Niña conditions; (B) Percentage of crop failure associated with maturity groups (MGs) in each region; (C) Percentage of crop failure associated with planting dates. Adapted from Hintz et al., (under preparation).

Discussion

This study offers insights for developing targeted strategies to mitigate soybean failure risk and improve productivity in regions vulnerable to WS in RS, Brazil. Although ENSO phases and planting dates were studied in Southern Brazil (Nóia Júnior et al., 2020), their interaction with MGs has not been explored yet. Since there are high uncertainties regarding in-season weather forecasts by the time management decisions are made by farmers, the integration of advanced weather forecasting and crop modeling tools can offer real-time insights and enhance decision-making processes. This research contributes to global efforts to enhance crop resilience by characterizing WS patterns in the face of climate uncertainty across several crops ; Battisti and Sentelhas, 2019).

Globally, climate variability is responsible for approximately a third of the yield variability. In important areas of the global breadbasket, it can account for up to 60% of the yield variability (Ray et al., 2015). Similar to findings by Sentelhas et al. (2015) in the same region, whom reported an average yield gap for soybeans of 1.6 Mg ha^{-1} due to water deficit, our study featured yield penalties up to 2 Mg ha^{-1} depending on the stress timing and severity. In this sense, environmental characterizations in regions highly affected by WS are crucial for breeding programs and future genotype-environment recommendations (Cooper et al., 2022; Resende et al., 2021). The results from our study point out that there is a regional yield variability across RS, being the SW the more susceptible to prolonged stress events (whole season stress, especially during La Nina), and the NE experiencing water stresses hardly ever. The yield penalizations due to La Nina phases towards the south of RS were also underscored by Nóia Júnior et al. (2020).

Effective risk management is crucial for agricultural decision-making, yet the adoption of quantitative predictive tools remains low due to barriers in knowledge transfer (Rose et al., 2016), and insufficient consideration of risk exposure and inherent uncertainties within production systems (Marra et al., 2003). The interactions among planting dates, cultivar maturity, and different ENSO phases present a strategic opportunity to reduce failure risk and mitigate yield penalties (Boer and Surmaini, 2020; Hammer et al., 2014; Ramirez-Rodrigues et al., 2014). Optimal maturity groups and planting dates vary with weather scenarios (Di Mauro et al., 2022; Nóia Júnior et al., 2020; Nóia Júnior and Sentelhas, 2019; Videla-Mensegue et al., 2024), underscoring the need for adaptive management strategies. For instance, Di Mauro et al. (2022), demonstrated that longer maturity groups were advantageous during La Niña phases in a similar region. Specifically, in the southernmost regions (SW and C), selecting longer maturity groups significantly reduced failure risk by approximately 15% during La Niña events. This highlights how variability in rainfall and temperature can substantially impact soybean yields (Ferreira and Rao, 2011).

Conclusions

Water stress was responsible for soybean yield penalties up to 2 Mg ha^{-1}. The NE region hardly ever experienced water stresses, while the SW region was more susceptible to prolonged stress events. Planting date and maturity group management adjustments resulted in over 15% reduction in crop failure. These findings offer valuable insights for developing targeted strategies to enhance soybean productivity and stability, thereby increasing the resilience of agricultural systems in the face of climate uncertainties.

References

Bates, D., Mächler, M., Bolker, B., Walker, S., 2015. Fitting Linear Mixed-Effects Models Using lme4. Journal of Statistical Software 67, 1–48. https://doi.org/10.18637/jss.v067.i01

Battisti, R., Sentelhas, P.C., 2019. Characterizing Brazilian soybean-growing regions by water deficit patterns. Field Crops Research 240, 95–105. https://doi.org/10.1016/j.fcr.2019.06.007

Boer, R., Surmaini, E., 2020. Economic benefits of ENSO information in crop management decisions: case study of rice farming in West Java, Indonesia. Theor Appl Climatol 139, 1435–1446. https://doi.org/10.1007/s00704-019-03055-9

Chapman, S.C., Cooper, M., Hammer, G.L., Butler, D.G., 2000. Genotype by environment interactions affecting grain

sorghum. II. Frequencies of different seasonal patterns of drought stress are related to location effects on hybrid yields. Aust. J. Agric. Res. 51, 209–222. https://doi.org/10.1071/ar99021

Chenu, K., Cooper, M., Hammer, G.L., Mathews, K.L., Dreccer, M.F., Chapman, S.C., 2011. Environment characterization as an aid to wheat improvement: interpreting genotype–environment interactions by modelling water-deficit patterns in North-Eastern Australia. Journal of Experimental Botany 62, 1743–1755. https://doi.org/10.1093/jxb/erq459

Conab - Portal de Informações Agropecuária [WWW Document], n.d. URL https://portaldeinformacoes.conab.gov.br/produtos-360.html (accessed 2.11.24).

Conab - Safra Brasileira de Grãos [WWW Document], n.d. URL https://www.conab.gov.br/info-agro/safras/graos (accessed 3.25.24).

Cooper, M., Messina, C.D., Tang, T., Gho, C., Powell, O.M., Podlich, D.W., Technow, F., Hammer, G.L., 2022. Predicting Genotype × Environment × Management (G × E × M) Interactions for the Design of Crop Improvement Strategies, in: Plant Breeding Reviews. John Wiley & Sons, Ltd, pp. 467–585. https://doi.org/10.1002/9781119874157.ch8

Di Mauro, G., Parra, G., Santos, D.J., Enrico, J.M., Zuil, S., Murgio, M., Zbinden, F., Costanzi, J., Arias, N., Carrio, A., Vissani, C., Fuentes, F., Salvagiotti, F., 2022. Defining soybean maturity group options for contrasting weather scenarios in the American Southern Cone. Field Crops Research 287, 108676. https://doi.org/10.1016/j.fcr.2022.108676

Ferreira, D.B., Rao, V.B., 2011. Recent climate variability and its impacts on soybean yields in Southern Brazil. Theor Appl Climatol 105, 83–97. https://doi.org/10.1007/s00704-010-0358-8

Fox, J., Weisberg, S., 2018. An R Companion to Applied Regression. SAGE Publications.

Fuentes-Llanillo, R., Telles, T.S., Soares Junior, D., de Melo, T.R., Friedrich, T., Kassam, A., 2021. Expansion of no-tillage practice in conservation agriculture in Brazil. Soil and Tillage Research 208, 104877. https://doi.org/10.1016/j.still.2020.104877

Funk, C., Peterson, P., Landsfeld, M., Pedreros, D., Verdin, J., Shukla, S., Husak, G., Rowland, J., Harrison, L., Hoell, A., Michaelsen, J., 2015. The climate hazards infrared precipitation with stations—a new environmental record for monitoring extremes. Sci Data 2, 150066. https://doi.org/10.1038/sdata.2015.66

Hammer, G.L., McLean, G., Chapman, S., Zheng, B., Doherty, A., Harrison, M.T., Oosterom, E. van, Jordan, D., 2014. Crop design for specific adaptation in variable dryland production environments. Crop Pasture Sci. 65, 614–626. https://doi.org/10.1071/CP14088

ISRIC — World Soil Information [WWW Document], n.d. . ISRIC — World Soil Information. URL https://www.isric.org (accessed 2.16.24).

Jeremy, G., 2023. geocmeans: An R package for spatial fuzzyc-means. JOSS 8, 5259. https://doi.org/10.21105/joss.05259

Nóia Júnior, R. de S., Fraisse, C.W., Karrei, M.A.Z., Cerbaro, V.A., Perondi, D., 2020. Effects of the El Niño Southern Oscillation phenomenon and sowing dates on soybean yield and on the occurrence of extreme weather events in southern Brazil. Agricultural and Forest Meteorology 290, 108038. https://doi.org/10.1016/j.agrformet.2020.108038

Nóia Júnior, R. de S., Sentelhas, P.C., 2019. Soybean-maize off-season double crop system in Brazil as affected by El Niño Southern Oscillation phases. Agricultural Systems 173, 254–267. https://doi.org/10.1016/j.agsy.2019.03.012

Pierre Pott, L., Jorge Carneiro Amado, T., Augusto Schwalbert, R., Mateus Corassa, G., Antonio Ciampitti, I., 2022. Crop type classification in Southern Brazil: Integrating remote sensing, crop modeling and machine learning. Computers and Electronics in Agriculture 201, 107320. https://doi.org/10.1016/j.compag.2022.107320

Poggio, L., de Sousa, L.M., Batjes, N.H., Heuvelink, G.B.M., Kempen, B., Ribeiro, E., Rossiter, D., 2021. SoilGrids 2.0: producing soil information for the globe with quantified spatial uncertainty. SOIL 7, 217–240. https://doi.org/10.5194/soil-7-217-2021

Ramirez-Rodrigues, M.A., Asseng, S., Fraisse, C., Stefanova, L., Eisenkolbi, A., 2014. Tailoring wheat management to ENSO phases for increased wheat production in Paraguay. Climate Risk Management 3, 24–38. https://doi.org/10.1016/j.crm.2014.06.001

Ray, D.K., Gerber, J.S., MacDonald, G.K., West, P.C., 2015. Climate variation explains a third of global crop yield variability. Nat Commun 6, 5989. https://doi.org/10.1038/ncomms6989

Resende, R.T., Piepho, H.-P., Rosa, G.J.M., Silva-Junior, O.B., e Silva, F.F., de Resende, M.D.V., Grattapaglia, D., 2021. Enviromics in breeding: applications and perspectives on envirotypic-assisted selection. Theor Appl Genet 134, 95–112. https://doi.org/10.1007/s00122-020-03684-z

Robertson, M.J., Carberry, P.S., Huth, N.I., Turpin, J.E., Probert, M.E., Poulton, P.L., Bell, M., Wright, G.C., Yeates, S.J., Brinsmead, R.B., 2002. Simulation of growth and development of diverse legume species in APSIM. Aust. J. Agric. Res. 53, 429–446. https://doi.org/10.1071/ar01106

Turek, M.E., Poggio, L., Batjes, N.H., Armindo, R.A., de Jong van Lier, Q., de Sousa, L., Heuvelink, G.B.M., 2023. Global mapping of volumetric water retention at 100, 330 and 15 000 cm suction using the WoSIS database. International Soil and Water Conservation Research 11, 225–239. https://doi.org/10.1016/j.iswcr.2022.08.001

Videla-Mensegue, H., Córdoba, M., Caviglia, O.P., Sadras, V.O., 2024. Soybean yield and water productivity gaps associate with ENSO-dependent effects of fungicide, sowing date and maturity group. European Journal of Agronomy 155, 127133. https://doi.org/10.1016/j.eja.2024.127133

Zuur, A.F., Ieno, E.N., Walker, N., Saveliev, A.A., Smith, G.M., 2009. Mixed effects models and extensions in ecology with R, Statistics for Biology and Health. Springer, New York, NY. https://doi.org/10.1007/978-0-387-87458-6